Design of Parallel-Jaw Gripper Tip Surfaces for Robust Grasping

Menglong Guo[1], David V. Gealy[1], Jacky Liang[2], Jeffrey Mahler[2],
Aimee Goncalves[1], Stephen McKinley[1], Ken Goldberg[3]

***Abstract*— Parallel-jaw robot grippers can grasp almost any object and are ubiquitous in industry. Although the shape, texture, and compliance of gripper jaw surfaces affect grasp robustness, almost all commercially available grippers provide a pair of rectangular, planar, rigid jaw surfaces. Practitioners often modify these surfaces with a variety of ad-hoc methods such as adding rubber caps and/or wrapping with textured tape. This paper explores a design space based on shape, texture, and compliance for gripper jaw surfaces. Over 37 jaw surface design variations were created using 3D printed casting molds and silicon rubber and tested with 1377 physical grasp experiments with a 4-axis robot (with automated reset). These tests evaluate grasp robustness as the probability that the jaws will acquire, lift, and hold a test set of objects at nominal grasp configurations computed by Dex-Net 1.0. Results suggest that a grid pattern with 0.03 inch void depth and 0.0375 inch void width on a silicone polymer with durometer of A30 yields grasp robustness that is 56% better than that of planar, rigid jaw surfaces [17, 29].**

I. Introduction

Robots operating in unstructured environments such as homes and warehouse order fulfillment centers may benefit from compliant end-effectors that are designed to successfully manipulate a wide variety of shapes and textures and resist torques due to contact and gravity [11]. Parallel-jaw grippers are widely used in the current generation of human-compliant robots, such as Sawyer from Rethink Robotics [31] or the YuMi from ABB [8], due to their low complexity, long lifetime, and ability to precisely manipulate objects [3]. Despite the intention that these robots be used in unstructured environments, most parallel-jaw grippers conform to the industrial paradigm of planar, rigid jaws [2].

One possible solution is to equip rigid parallel-jaw grippers with compliant or high-friction finger pads. A variety of designs have been proposed such as gecko-inspired microstructures [12], polymer pancakes [7], and human-inspired skin, bone, and nail structures [17, 29]. The design process for these compliant fingers has been largely guided by human intuition and optimization in simulation [4], and often only one or a small number of designs have been physically realized due to the time and material cost of manufacturing. However, the gripper/object surface interaction is difficult to model and predict in simulation; thus, a design method involving physical robot testing and rapid prototyping is advantageous for developing a more successful gripper.

[1]University of California, Berkeley, Mechanical Engineering;
{m.guo, dgealy, mckinley}@berkeley.edu
[2]University of California, Berkeley, EECS;
{jackyliang, jmahler}@berkeley.edu
[3]University of California, Berkeley, IEOR & EECS;
goldberg@berkeley.edu
The AUTOLAB at UC Berkeley (automation.berkeley.edu)

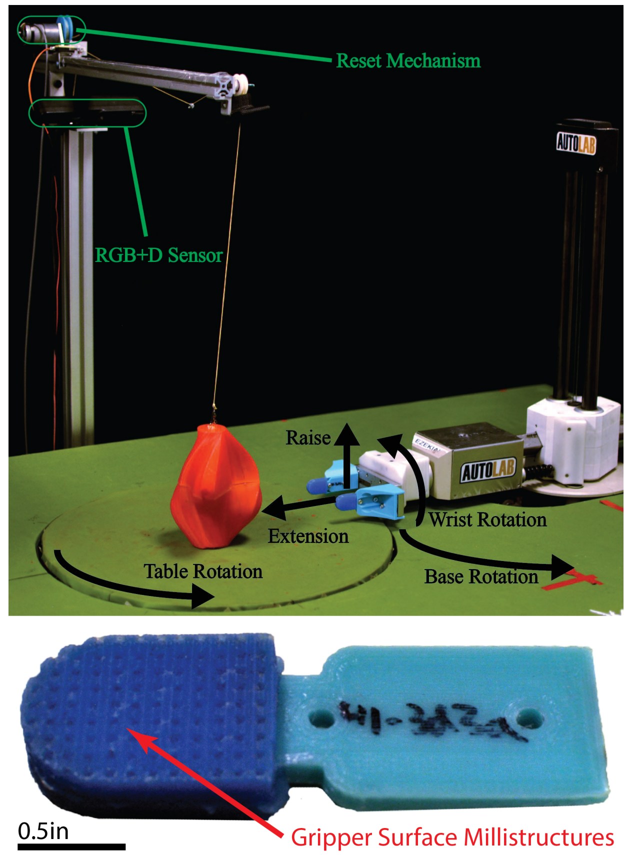

Fig. 1: **Above:** Probability of success for gripper surfaces was empirically studied on the Zymark Robot with 4 degrees of freedom plus a binary gripper and rotating turntable. The test objects were identified by a PrimeSense Camera and rotated into position for gripping. A reset mechanism lifts and replaces each object to the center of the table after each grasp trial. **Below:** Gripper surface millistructures were cast in silicone polymer using a 3D printed mold.

Inspired by recent advances in 3D printing and rapid prototyping, we explored the possibility of guiding the design process empirically, evaluating success on a physical system for a large number of prototype fingertip designs. Our primary contribution is an evaluation of gripper surface texture and stiffness for compliant robotic fingers (as shown in dark blue in Figure 1) across 37 iterations of individual conceptual surface features (as shown in Figure 5). Each design was parametrized and prototyped using 3D printing and molded silicone. Inspired by zooming optimization methods [21] we iteratively evaluated the probability of grasp success for our design set and expanded our design set around the most promising design from the previous evaluations. We collected between 21 and 35 grasp trials for each design across three 3D printed objects on a Zymark Zymate robot for a total of 1377 total evaluations. The resulting design's probability of success improved by 56% compared to that of the original planar rigid jaw surface gripper.

Initial Assumptions: The Series Type A Pro 3D printers extrude Polylactic Acid (PLA). Platinum-cure silicon rubber was used for a compliant material because it is robust, easy to manufacture and can be washed. Grasps were tested with a Zymark Zymate 2 laboratory robot with positional uncertainty of up to $5mm$ and a pointcloud-based vision system with positional error of up to $1mm$. Known objects from the Dex-Net 1.0 dataset [25] were used to test grasps on a parallel-jaw laboratory robot [25].

II. Related Work

A. Related work in gripper design

An important tool for design inspiration is the idea of utilizing nature as a model; this holds true for robotic gripper design. Two specific areas this design concept has been applied to are structural and surface features.

Structurally, a typical robotic finger consists of a single, uniform, rigid material throughout, regardless of its shape. However, anthropomorphic observations reveal that human fingers consist of several layers: bone, soft tissue, skin, and nails, where each of these characteristics provide a unique function for human grasping. To increase the ability of a robotic hand, Murakami et al. [29] explored adding a hard nail with a strain gauge to a fingertip covered by soft elastic. Hosoda et al. explored these characteristics as well by using a metal bar and two types of silicone rubber to replicate the bone-body-skin structure [17]. Randomly embedded strain gauges were added into the silicone to replicate sense of touch. To study the benefits of compliance on surface contact gripping, Berselli et al. designed and tested soft fingertip covers with four varied internal geometric structures. Rapid prototyping was utilized for inexpensive fingertip production [1]. These designs revealed the effectiveness of utilizing multiple materials for manipulation.

Numerous nature-inspired surface features have been investigated for their various attractive properties. Initially motivated by the fingerprint surfaces on human hands, Cutkosky et al. found that textured and compliant gripper surfaces improved object handling [9]. Several materials were tested under dry, clean conditions and wet, dirty conditions to test their adhesive and friction properties. Expanding on their study of bio-inspired adhesive materials, Cutosky et al. analyzed the pads on gecko toes for load sharing [12]. Their study found non-uniform stress distribution over gecko lamellae, suggesting uneven load-sharing over gecko toe pads.

Gecko-inspired adhesives have been developed to replicate the strong adhesion geckos possess, both as sheets and as gripper surfaces. Hawkes et al. developed grippers that use shear adhesion of gecko inspired fibrillar film micro-structures to grasp curved objects [15]. Similar structures have been used for adhesion on treaded robots [28]. While efficacy of these structures diminishes at greater payload because required density of micro-structures increases with payload (ie: geckos are 100g and need 10000 hairs per mm squared), these bio-inspired surfaces have proven effective on small payloads [13].

In addition to material selection, it has been suggested that interface geometry is important for adhesion. To try and provide insight on adhesion mechanisms like that of the gecko, uniform surface patterns were explored by Crosby et al. [7]. Described as polymer 'pancakes', tests were run for surfaces with a range of cylindrical posts with varying heights, diameters, and grid-spacing. These patterned dimensions were linked to material properties which increase grip force for sliding contact; from this, adhesion effect relationships were extracted between surface dimensions and material properties. This conceptual surface feature inspired initial design concepts in Section III.

Fig. 2: The design space for fingertip surfaces was explored over 37 different physical iterations using methods inspired by machine learning optimization techniques. Here are all of the molds (white objects) fingertips produced during design exploration.

B. Optimization Methods

This work is also closely related to work on optimization methods for gripper design. While much research has relied on intuition and exact parametric models to guide gripper design, recent research has considered convex optimization of gripper parameters when such a parametrization is available. Ciocarlie et al. [4] formulated the optimization of actuation mechanisms for an under-actuated hand as a convex quadratic program. Dollar and Howe [10] optimized the joint coupling parameters of an under-actuated hand by solving a system of equations.

However, many design problems have more than one locally optimal solution. Methods for non-convex optimization are difficult to apply in design because of the limited opportunity to iterate on physical prototypes. A common technique in robotics is simulated annealing [19], which has been used extensively in grasp planning [6]. Shalaby et al. [34] used simulated annealing to optimize the topology of a compliant gripper. Ciocarlie et al. [5] used a modified

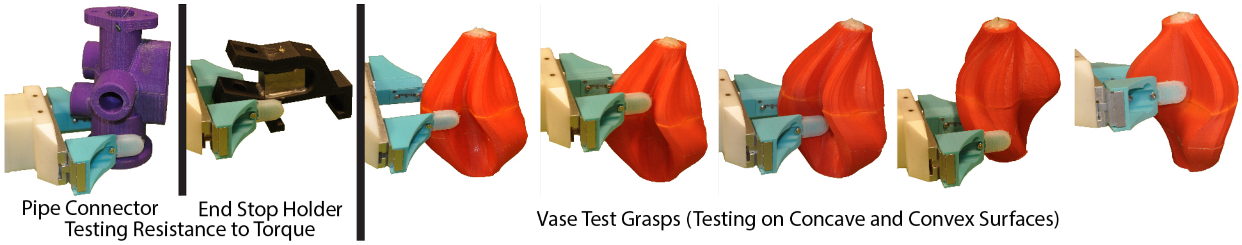

Fig. 3: The grasping dataset was chosen from available models created by users of the online part database 'Thingiverse'. These seven grasps were chosen to highlight the success of a gripper in an unstructured environment. The 'Pipe Connector' and 'End Stop Holder' were chosen to specifically investigate resistance to torque over curved and flat surfaces. The 'Vase' object was chosen because of its convex and concave surfaces.

form of gradient descent to optimize the kinetic behavior of a two-finger gripper. Similar methods include nonlinear programming for parallel jaw gripper design [36], evolutionary algorithms [32], and sequential convex programming for kinematic design of two finger grippers [24].

Our approach to exploring a design space is inspired by these optimization techniques. However, we considered using success on a physical instantiation of grasping to guide the design process rather than using a parametric approximation (see 3). This was done to avoid accumulating errors in design due to errors in modeling and simulation. However, uncertainty in physical trials could introduce noise into successful evaluations, requiring multiple samples.

Past research on this topic in robotics has focused on optimizing a sampled estimate of the objective, for example in policy gradients for locomotion [33] or sampling for robust grasp planning [18, 20]. However, this may require many samples to converge for each prototype. Methods to minimize iterations during optimization include Multi-Armed Bandits (MABs) [23, 25] and Bayesian Optimization (BO) [16, 26, 27, 35], which allocate fewer samples to regions with a high likelihood of being suboptimal based on samples collected.

Standard realizations of MAB and BO methods would require a predefined set of designs to optimize. However, we desired to allocate manufacturing effort only to more promising designs with higher success rates. Thus, our method was inspired by zooming methods [22], where the optimization approach iteratively resampled the space at finer resolution in more promising regions. Recently, Kleinberg et al. [21] developed a zooming algorithm for solving the MAB problem over L-Lipschitz metric spaces. In comparison, we iteratively evaluated the success for a fixed set of designs using a uniform allocation strategy on a physical robot. Then we resampled the design set around the design with the highest sample mean for the next round of evaluation as discussed in Section IV.

III. Problem Formulation

We consider the problem of finding a parallel-jaw fingertip design that maximizes the likelihood that a grasp is successful on a physical system. We assume that the probability of success for a particular design and grasp is stationary; e.g. the robot's control and perception calibration is constant over time.

Our design problem had the following attributes: probability of success could be determined quickly through experimental trials, fabrication could be iterated quickly using rapid prototyping, and the space of parameters was relatively small. We note that our empirical design approach can only be expected to work in design problems with similar complexity to that of the fingertip design discussed in this paper, limited by the size of the design space as well as time for fabrication and testing.

Our objective was to maximize the mean likelihood of success for grasps in our test set over a space of possible designs, which we formalize below for concreteness.

A. Design Space

Let $\mathcal{D}$ be the *design space*, a set of parameters specifying all possible designs. For example, $\mathcal{D} \subset \mathbb{Z} \times \mathbb{R}$ could represent the width of dots and depth of the fingertip surface structures. We assumed the design space is bounded and fixed. We called an element $d \in \mathcal{D}$ a design.

B. Object and Parallel-Jaw Grasping Model

Let $\mathcal{O}$ be an object to grasp with center of mass $\mathbf{z} \in \mathbb{R}^3$. For clarity, we assumed the vertices of the mesh are specified with respect to a reference frame $T_{\mathcal{O}} = (R_{\mathcal{O}}, \mathbf{t}_{\mathcal{O}}) \in SE(3)$ centered on $\mathbf{z}$ and oriented along the principal axes of the object [25].

We parametrized parallel-jaw grasps as $\mathbf{g} = (\mathbf{x}, \mathbf{v}, \theta)$ where $\mathbf{x} \in \mathbb{R}^3$ is the grasp center, $\mathbf{v} \in \mathcal{S}^2$ is the grasp axis, and $\theta \in \mathcal{S}$ is the approach angle. We assumed randomness in executing a particular grasp on a given object, which may occur due to imprecision in sensing and actuation.

Let $\Gamma = \{(\mathbf{g}_1, \mathcal{O}_1), ..., (\mathbf{g}_n, \mathcal{O}_n)\}$ be a given set of test grasps and objects. For example Γ could contain grasps sampled from the handles on a set of industrial parts.

C. Design Objective

Let $S_i(d)$ be a binary random variable measuring the success of using design d to execute grasp $\mathbf{g}_i$ on $\mathcal{O}_i$. Our goal was to find the design that maximizes the mean likelihood of success for grasps in our test set (shown in Figure 3):

$$d^* = \operatorname*{argmax}_{d \in \mathcal{D}} \frac{1}{n} \sum_{i=1}^{n} \mathbb{P}\left(S_i(d) = 1\right) \tag{1}$$

which is the expected number of successes for a uniform distribution over the dataset Γ.

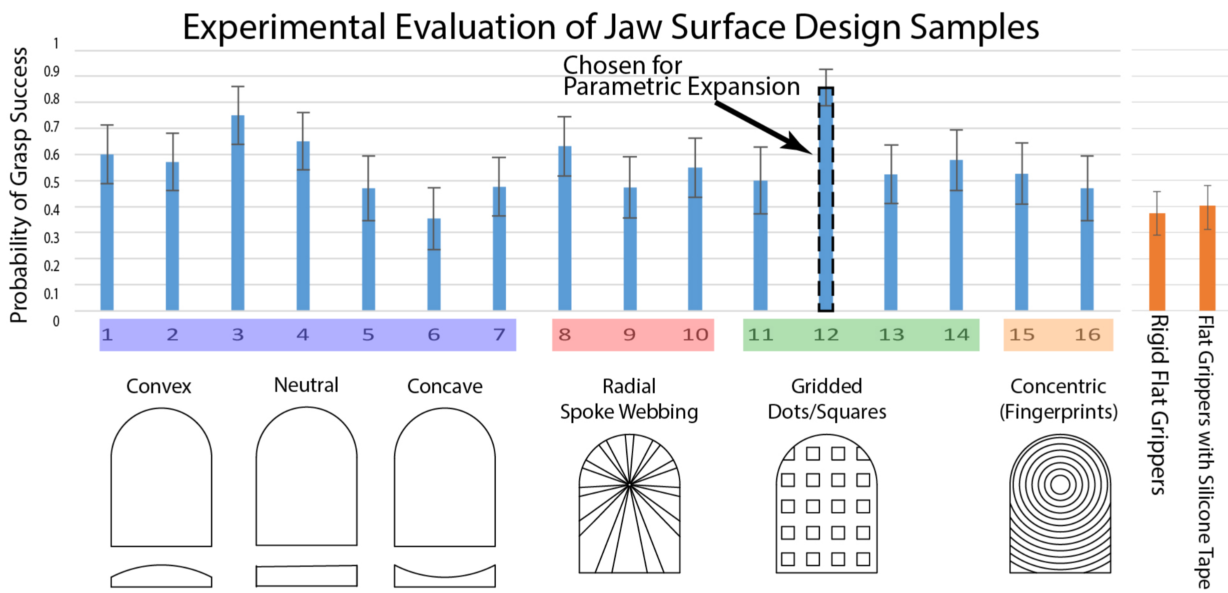

Fig. 4: Initial explorations for gripper surfaces were made for each conceptual design based on related work and the manufacturing limits of the 3D printers. Initial designs were compared against default rigid grippers and grippers covered in adhesive tape (as shown in orange at right).

D. Methodology

Solving Equation 1 may be very difficult in practice due to the large number of possible designs, grasps, and objects. Our approach to this problem was inspired by zooming methods in optimization [21, 22]. We first formed an initial discrete set of designs sampled from a number of concepts, such as different surface features and fingertip geometries. We then evaluated the probability of success for all designs on all grasps and objects in our test set by sampling. Specifically, we estimated the probability of success by taking the percentage of successes over m total trials

$$P_S(d, \mathbf{g}_i, \mathcal{O}_i) = \frac{1}{m} \sum_{j=1}^{m} \mathbf{1}(\hat{S}_{i,j}(d) = 1)$$

where $\hat{S}_{i,j}(d)$ is the j-th sample of $S_i(d)$ and $\mathbf{1}(\cdot)$ is the indicator function. We then expanded our design set by sampling a grid of design parameters around the best performing design from the initial set. Finally, we repeatedly evaluated and resampled for k rounds, choosing the design with the highest sample mean as $\hat{d}^*$ at termination. We used $k = 3$ and $m = 3$ in our experiments based on the amount of time to run each trial and round of evaluations.

IV. Experimental Evaluation

A. Fabrication of Gripper Surfaces

Molds were created with *Series 1 Pro Type A* 3D printers from Polylactic acid (PLA) filament. This manufacturing step limited the resolution of surface textures to 0.1 mm. On the parallel jaws of the robot, 3D printed mounts allowed for quick swapping of grippers for testing and minimized the development cost per iteration. Each gripper had an identical base printed from PLA filament to index into the mount. The base served as a hard plastic structure for the soft silicone rubber tips to be cast around. The unique texture surface was created by casting the base in 3D printed molds shown in Figure 5.

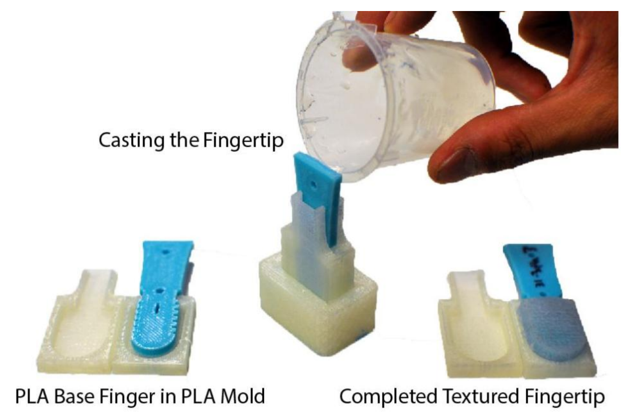

Fig. 5: Fingertips were cast around a PLA 'bone' structure at the center of each finger. Mold components were 3D printed from PLA.

TABLE I: Silicone Rubber Properties (Manufactured by Smooth-On)

Silicone Rubber	Softness (Durometer)	Stiffness (Elongation at Break %)
Mold Star 30	30A	339%
Dragon Skin 30	30A	364%
Dragon Skin 10	10A	1000%
Eco Flex 00-20	00-20	845%

B. Dataset

Our design test set Γ consisted of seven total grasps across three objects, illustrated in Fig. 3. The dataset was selected to test (a) resistance to torques about the principle grasp axis, which are difficult to resist with two fingers [2], and (b) adaptivity to varying geometric features such as concavities, convexities, and ridges.

The two grasps on the end stop holder and pipe connector were chosen to test (a) torque resistance and the five grasps on the vase were chosen to test (b) geometric adaptivity. Each object was also labeled with a single stable pose on the table chosen for reachability with our 4 degree of freedom arm. All grasps were hand-selected from a set of contact points generated using the antipodal grasp sampling of Dex-Net 1.0 [25], and the approach axis was constrained to be parallel to the table for the given stable pose.

C. Experimental Platform

Grasping trials were run on a Zymark Zymate 2 robot with 4 degrees of freedom plus gripper control and a rotating turntable for 5 total controllable degrees of freedom (as shown in Figure 1). To begin an experiment, a test object was placed onto the workspace table in a pre-defined stable pose and attached to a reset mechanism. For each grasp trial, a PrimeSense Carmine 1.09 depth sensor was used to register the pose of the object. After registration, the robot proceeded to perform a chosen grasp by planning a straight line trajectory to the desired grasp pose, moving to the pose, and closing its jaws. The robot then attempted to raise the object by 17.5mm, at which point the PrimeSense camera took a color picture for labeling. This concluded a single trial. To begin the next trial, the reset mechanism then raised and lowered the test object back to the known stable pose on the work table.

Registration was performed using convolutional neural networks for a coarse pose estimate [14] and Iterated Closest Point matching with a weighted point-to-plane objective [30] for fine pose estimation in the plane of the table. The registration system had a mean X translational error of 4.2mm, a mean Y translational error of 1.0 mm, and a mean angular error of $5.1°$ in the plane. The standard deviations were 3.1mm, 3.3mm, and $8.6°$ for X translation, Y translation, and rotation in the plane, respectively.

Fig. 6: Success and failures were hand labeled and fell into several categories. A drop failure occurred when the gripper failed to hold the object. A slip occurred when the gripper could not resist gravitational torque and rotated 10 degrees below horizontal. A cage failure occurred when the lift was successful despite positional errors.

D. Grasp Success Criteria

Each grasp was considered a success or failure based on the criteria illustrated in Fig. 6. We considered a grasp attempt a failure if it fell into one of three modes:

1) **Drop:** The gripper failed to lift the object.
2) **Slip:** The gripper lifted the object but the object rotated by more than 10 degrees about the principle grasp axis.
3) **Cage:** The gripper lifted the object upright but leveraged a part of the gripper other than the fingertip surface.

Therefore a grasp was considered successful if it lifted the object in an upright position using only the fingertips.

To provide labels for each grasp, we collected a single image of the grasp after the arm had attempted to lift the object for each grasp trial. Then, a single human labeler was shown the image of each grasp and asked to label the grasp as a success or failure based on the above criteria or reject the datapoint. Datapoints were rejected if the robot pushed the object out of the way and thus failure could not be attributed to the fingertips themselves.

V. Design Evaluation

The study included $k = 3$ rounds of design evaluation. Our design space $\mathcal{D}$ consisted of the following parameters: curvature of the fingertip, angular resolution of spoke webbing patterns, radial resolution of concentric patterns, fingertip softness, and depth, shape, and width of gridded fingertip indentations. The cross-sectional dimensions of the fingertip were modeled after the dimensions of the human thumb (width $= 0.8$in, height $= 1.1$in, and depth $= 0.35$in).

A. Initial Design Concepts

Initial design concepts were chosen to reflect a study of related works (Section II). Designs were intended to maximally resist torque around the fingertip surface. Concepts 1 through 7 (as shown in Figure 4) were parametrized by radius of surface curvature (radius = 0.93, 1.36, 2.68, flat, -2.68, -1.36, -0.93 in). Concepts 8 through 16 (as shown in Figure 4) are parametrized by width of surface features, distance between features, and depth of the surface features. For each design, we evaluated each of the 7 grasps in Fig. 3 for $m = 3$ for a total of 21 binary success trials per design. As a baseline, standard rigid flat grippers and flat grippers with silicone tape underwent the same evaluation (Fig. 4). Design 12, which had a grid of square surface indentations reminiscent of a waffle, had an 86% probability of success and was chosen for expansion.

B. First Parametrized Expansion

In the second round, a 3x3x3 grid-search was employed to explore the parametric design space near initial design 12. These 27 design permutations investigated the relationship between gripper stiffness (elongation at 100% strain), void depth, and void width.

Parameters Explored:

Materials: Dragon Skin 30 (DS30), Mold Star 30 (MS30), and a 50:50 mixture between DS30 and MS30.

Void Width: 0.03 0.0375 0.045 in.

Void Depth: 0.03, 0.05, 0.07 in.

Again, for each design we evaluated each of the 7 grasps in Fig. 3 for $m = 3$ samples. The results of the second round are illustrated in Fig. 7. The results suggest that lower stiffness materials and shallower indentation depth performed better. The best performing design had the same indentation depth and width as design 12 with lower stiffness, which had a 90% probability of success.

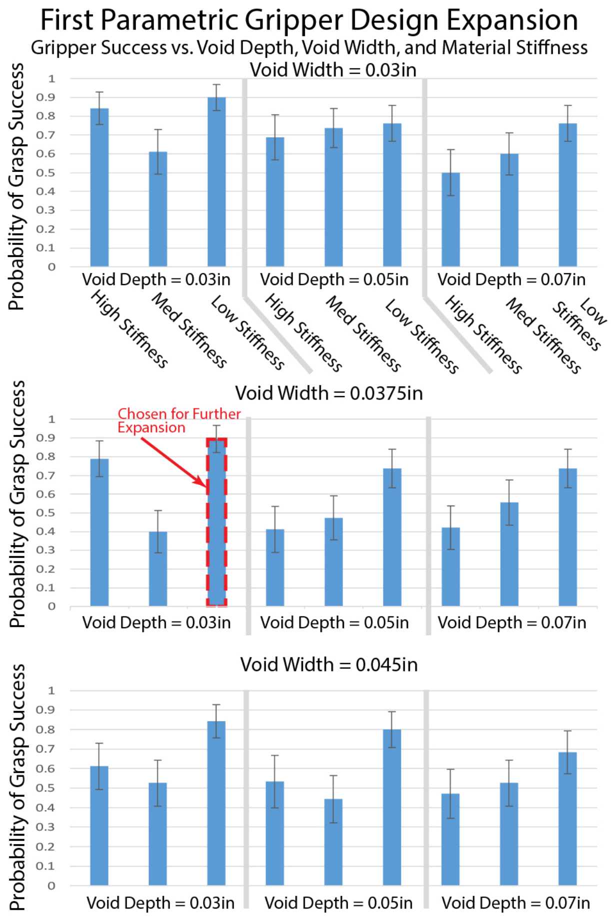

Fig. 7: The first round of parametric expansion investigates the effect of material stiffness, void depth, and void width on the most successful design from the initial set (shown in Figure 4) through a 3x3x3 cube of possibilities. Success was found to be linked to lower stiffness and diminished void width.

C. Second Parametrized Expansion

In the second expansion, we investigated the square indented gripper with further exploration of void depth. We also explored material softness.

Parameters Explored:

Materials: Dragon Skin 30, Dragon Skin 10, Eco-Flex 00-20.
Void Depth: 0.02, 0.03 in.

We were forced to use a backup Zymark robot in our design evaluations because the robot we tested on in the first two rounds malfunctioned. Thus, we ran the same 7 grasps but with $m = 5$ samples each instead of 3 because we found that the backup robot was noisier and we needed to reject more samples for each design. The results are illustrated in Fig.8. We found that further softening the material and reducing the depth of the indentations decreased the probability of success. Furthermore, all designs had a lower probability of success on the backup robot.

The most successful design $\hat{d}^*$ was the winner of round two, which had an void depth of 0.03in, an void width of 0.0375in, and a durometer of A30.

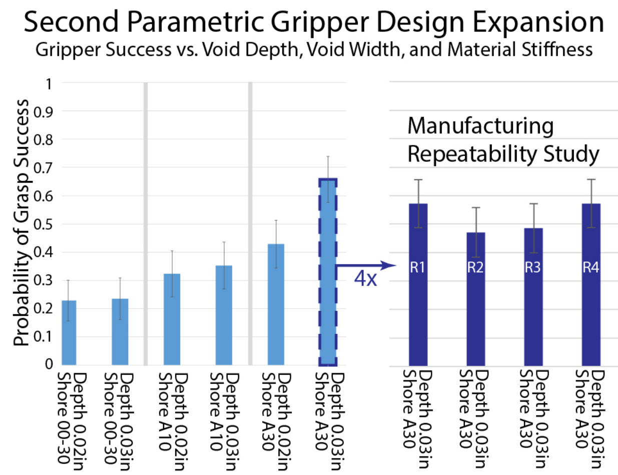

Fig. 8: A second round of parametric expansion further explored the effect of smaller void depth and material softness on grasping success. The most successful design was fabricated four more times and tested on the same conditions to verify manufacturing repeatability (shown at right in dark blue).

D. Manufacturing Repeatability

We made 4 additional copies of $\hat{d}^*$ and evaluated the probability of success for each independently in order to measure the repeatability of our manufacturing process. The results are illustrated in the right panel of Fig. 8. We found that the designs have different success probabilities ranging from 47% to 65% with a mean of 55% and a standard deviation of approximately 7%. This suggests that variability in our manufacturing process affects the success of the design. However, even in the worst case the design had a higher estimated success probability than the other designs in second round.

E. Manufacturing and Evaluation Time

The whole process to create 16 unique grippers in round one took approximately 11.5 hours. Printing the base took 1.5 hours, printing the 2 molds for each gripper took 4 hours, casting silicone took 4 hours to solidify, and setup of the printing process took 1 hour. We parallelized printing over several printers in order to reduce the total manufacturing time. Each grasp took approximately 1.5 minutes to execute. With 1377 total grasps, the total time was 31 hours. While the total time to evaluate 35 grasps was approximately 50 minutes, the reset mechanism allowed us to run the tests autonomously and the human only needed to intervene to change the fingertips and objects. Thus, the operator only needed to perform approximately 2 hours of actual work across the experiments for all rounds.

VI. Discussion and Future Work

We evaluated gripper surface texture and stiffness for compliant robotic fingertips across 37 iterations of individual conceptual surface features and 1377 grasping evaluations to determine the surface feature with the highest probability of success compared to standard planar, rigid jaw surfaces.

We do not claim to have found the optimal gripper in this space; however, our process systematically searches the design space for more successful instantiations. Our initial baselines were a flat gripper and a flat gripper wrapped with silicone tape (an industry standard). After testing these baselines through our grasp dataset (shown in Fig. 3), the probability of success was 37% and 40% respectively (as shown in Fig. 4). At the end of the process, the best gripper yielded 67% (see Fig. 8).

Exploiting this design approach, we want to combine these grippers with embedded force sensors and explore various fingertip surface textures and their effects on the sensing system's sensitivity to shear forces.

In the future, we want to test this process and these gripper designs on robots with more degrees of freedom to optimize for previously unreachable grasps and objects. We also plan on implementing multi-armed bandits on the process to reduce the number of iterations it takes to determine the most successful gripper.

Acknowledgements

This research was performed at the AUTOLAB at UC Berkeley in affiliation with the AMP Lab, BAIR, and the CITRIS 'People and Robots' Initiative (CPAR): (robotics.citris-uc.org). This work was supported in part by the U.S. National Science Foundation under NRI Award IIS-1227536: Multilateral Manipulation by Human-Robot Collaborative Systems; and by Google and Cisco.

The authors were supported in part by the U.S. National Science Foundation under NRI Award IIS-1227536: Multilateral Manipulation by Human-Robot Collaborative Systems, by the Department of Defense (DoD) through the National Defense Science & Engineering Graduate Fellowship (NDSEG) Program, and by Google, Cisco, Siemens, Cloudminds.

Any opinions, findings, and conclusions or recommendations expressed in this material are those of the authors and do not necessarily reflect the views of the sponsors. We thank our colleagues who provided helpful feedback and suggestions, in particular Animesh Garg, Michael Laskey, and Sanjay Krishnan.

REFERENCES

[1] G. Berselli and G. Vassura, "Differentiated layer design to modify the compliance of soft pads for robotic limbs," in *Robotics and Automation, 2009. ICRA'09. IEEE International Conference on*. IEEE, 2009, pp. 1285–1290.

[2] A. Bicchi and V. Kumar, "Robotic grasping and contact: A review," in *IEEE International Conference on Robotics and Automation*. Citeseer, 2000, pp. 348–353.

[3] A. Bicchi and A. Marigo, "Dexterous grippers: Putting nonholonomy to work for fine manipulation," *The International Journal of Robotics Research*, vol. 21, no. 5-6, pp. 427–442, 2002.

[4] M. Ciocarlie and P. Allen, "A constrained optimization framework for compliant underactuated grasping," *Mech. Sciences*, vol. 2, no. 1, pp. 17–26, 2011.

[5] M. Ciocarlie, F. M. Hicks, R. Holmberg, J. Hawke, M. Schlicht, J. Gee, S. Stanford, and R. Bahadur, "The velo gripper: A versatile single-actuator design for enveloping, parallel and fingertip grasps," *The International Journal of Robotics Research*, vol. 33, no. 5, pp. 753–767, 2014.

[6] M. T. Ciocarlie and P. K. Allen, "Hand posture subspaces for dexterous robotic grasping," *The International Journal of Robotics Research*, vol. 28, no. 7, pp. 851–867, 2009.

[7] A. J. Crosby, M. Hageman, and A. Duncan, "Controlling polymer adhesion with pancakes," *Langmuir*, vol. 21, no. 25, pp. 11 738–11 743, 2005.

[8] P. Crowther, "Yumi® irb 15000 overview," https://library.e.abb.com/public/4bcf2603f76f49088b80f7f1c49045eb/IRB14000ExternalVersionFinal.pdf, 2015.

[9] M. Cutkosky, J. Jourdain, and P. Wright, "Skin materials for robotic fingers," in *Robotics and Automation. Proceedings. 1987 IEEE International Conference on*, vol. 4. IEEE, 1987, pp. 1649–1654.

[10] A. M. Dollar and R. D. Howe, "Joint coupling design of underactuated grippers," in *ASME 2006 International Design Engineering Technical Conferences and Computers and Information in Engineering Conference*. American Society of Mechanical Engineers, 2006, pp. 903–911.

[11] ——, "The highly adaptive sdm hand: Design and performance evaluation," *The international journal of robotics research*, vol. 29, no. 5, pp. 585–597, 2010.

[12] E. V. Eason, E. W. Hawkes, M. Windheim, D. L. Christensen, T. Libby, and M. R. Cutkosky, "Stress distribution and contact area measurements of a gecko toe using a high-resolution tactile sensor," *Bioinspiration & biomimetics*, vol. 10, no. 1, p. 016013, 2015.

[13] S. N. Gorb, M. Sinha, A. Peressadko, K. A. Daltorio, and R. D. Quinn, "Insects did it first: a micropatterned adhesive tape for robotic applications," *Bioinspiration & biomimetics*, vol. 2, no. 4, p. S117, 2007.

[14] S. Gupta, R. Girshick, P. Arbeláez, and J. Malik, "Learning rich features from rgb-d images for object detection and segmentation," in *European Conference on Computer Vision*. Springer, 2014, pp. 345–360.

[15] E. W. Hawkes, D. L. Christensen, A. K. Han, H. Jiang, and M. R. Cutkosky, "Grasping without squeezing: Shear adhesion gripper with fibrillar thin film," in *2015 IEEE International Conference on Robotics and Automation (ICRA)*. IEEE, 2015, pp. 2305–2312.

[16] G. Hitz, A. Gotovos, M.-É. Garneau, C. Pradalier, A. Krause, R. Y. Siegwart, *et al.*, "Fully autonomous focused exploration for robotic environmental monitoring," in *2014 IEEE International Conference on Robotics and Automation (ICRA)*. IEEE, 2014, pp. 2658–2664.

[17] K. Hosoda, Y. Tada, and M. Asada, "Anthropomorphic robotic soft fingertip with randomly distributed receptors," *Robotics and Autonomous Systems*, vol. 54, no. 2, pp. 104–109, 2006.

[18] K. Hsiao, M. Ciocarlie, and P. Brook, "Bayesian grasp planning," in *ICRA 2011 Workshop on Mobile Manipulation: Integrating Perception and Manipulation*, 2011.

[19] C.-R. Hwang, "Simulated annealing: theory and applications," *Acta Applicandae Mathematicae*, vol. 12, no. 1, pp. 108–111, 1988.

[20] B. Kehoe, D. Berenson, and K. Goldberg, "Toward cloud-based grasping with uncertainty in shape: Estimating lower bounds on achieving force closure with zero-slip push grasps," in *Proceedings of the IEEE International Conference on Robotics and Automation*. IEEE, 2012, pp. 576–583.

[21] R. Kleinberg, A. Slivkins, and E. Upfal, "Multi-armed bandits in metric spaces," in *Proceedings of the fortieth annual ACM symposium on Theory of computing*. ACM, 2008, pp. 681–690.

[22] Y.-D. Kwon, S.-B. Kwon, S.-B. Jin, and J.-Y. Kim, "Convergence enhanced genetic algorithm with successive zooming method for solving continuous optimization problems," *Computers & Structures*, vol. 81, no. 17, pp. 1715–1725, 2003.

[23] T. L. Lai and H. Robbins, "Asymptotically efficient adaptive allocation rules," *Advances in applied mathematics*, vol. 6, no. 1, pp. 4–22, 1985.

[24] C. Lanni and M. Ceccarelli, "An optimization problem algorithm for kinematic design of mechanisms for two-finger grippers," *Open Mechanical Engineering Journal*, vol. 3, pp. 49–62, 2009.

[25] J. Mahler, F. T. Pokorny, B. Hou, M. Roderick, M. Laskey, M. Aubry, K. Kohlhoff, T. Kröger, J. Kuffner, and K. Goldberg, "Dex-net 1.0: A cloud-based network of 3d objects for robust grasp planning using a multi-armed bandit model with correlated rewards," *ICRA*, 2016.

[26] R. Marchant and F. Ramos, "Bayesian optimisation for intelligent environmental monitoring," in *2012 IEEE/RSJ International Conference on Intelligent Robots and Systems*. IEEE, 2012, pp. 2242–2249.

[27] R. Martinez-Cantin, N. de Freitas, E. Brochu, J. Castellanos, and A. Doucet, "A bayesian exploration-exploitation approach for optimal online sensing and planning with a visually guided mobile robot," *Autonomous Robots*, vol. 27, no. 2, pp. 93–103, 2009.

[28] C. Menon, M. Murphy, and M. Sitti, "Gecko inspired surface climbing robots," in *Robotics and Biomimetics, 2004. ROBIO 2004. IEEE International Conference on*. IEEE, 2004, pp. 431–436.

[29] K. Murakami and T. Hasegawa, "Novel fingertip equipped with soft skin and hard nail for dexterous multi-fingered robotic manipulation," in *Robotics and Automation, 2003. Proceedings. ICRA'03. IEEE International Conference on*, vol. 1. IEEE, 2003, pp. 708–713.

[30] R. A. Newcombe, A. J. Davison, S. Izadi, P. Kohli, O. Hilliges, J. Shotton, D. Molyneaux, S. Hodges, D. Kim, and A. Fitzgibbon, "Kinectfusion: Real-time dense surface mapping and tracking," in *IEEE Int. Symp. on Mixed and augmented reality (ISMAR)*. IEEE, 2011, pp. 127–136.

[31] rethink robotics, "Sawyer user guide for intera 3.3 software," http://mfg.rethinkrobotics.com/mfg-mediawiki-1.22.2/images/1/1a/Sawyer_User_Guide_3.3.pdf, 2016.

[32] R. Saravanan, S. Ramabalan, N. G. R. Ebenezer, and C. Dharmaraja, "Evolutionary multi criteria design optimization of robot grippers," *Applied Soft Computing*, vol. 9, no. 1, pp. 159–172, 2009.

[33] J. Schulman, S. Levine, P. Moritz, M. I. Jordan, and P. Abbeel, "Trust region policy optimization," *CoRR, abs/1502.05477*, 2015.

[34] M. M. Shalaby, H. A. Hegazi, A. O. Nassef, and S. M. Metwalli, "Topology optimization of a compliant gripper using hybrid simulated annealing and direct search," in *ASME 2003 International Design Engineering Technical Conferences and Computers and Information in Engineering Conference*. American Society of Mechanical Engineers, 2003, pp. 641–648.

[35] J. Snoek, H. Larochelle, and R. P. Adams, "Practical bayesian optimization of machine learning algorithms," in *Advances in neural information processing systems*, 2012, pp. 2951–2959.

[36] T. Zhang and K. Goldberg, "Design of robot gripper jaws based on trapezoidal modules," in *Robotics and Automation, 2001. Proceedings 2001 ICRA. IEEE International Conference on*, vol. 2. IEEE, 2001, pp. 1065–1070.